CTH-IEFT/PP-1996-15

ISSN 0

Stability of ideal and resistive modes in cylindrical plasmas with resistive walls and plasma rotation

A. Bondeson and H. X. Xie

INSTITUTIONEN FÖR ELEKTROMAGNETISK FÄLTTEORI
CHALMERS TEKNISKA HÖGSKOLA

INSTITUTE FOR ELECTROMAGNETIC FIELD THEORY AND PLASMA PHYSICS

CHALMERS UNIVERSITY OF TECHNOLOGY
GOTHENBURG, SWEDEN

Stability of ideal and resistive modes in cylindrical plasmas with resistive walls and plasma rotation

A. Bondeson[a]

Institute of Electromagnetic Field Theory, Euratom-NFR/Fusion Association, Chalmers University of Technology, S-412 96 Göteborg, Sweden

H. X. Xie

Department of Technology, Euratom-NFR/Fusion Association, Uppsala University, Box 534, S-751 21 Uppsala, Sweden

Abstract

The stabilization of cylindrical plasmas by resistive walls combined with plasma rotation is analyzed. Perturbations with a single mode rational surface $q = m/n$ in a finitely conducting plasma are treated by the "resistive kink" dispersion relation of Coppi *et al* [Sov. J. Plasma Phys. **2**, 533 (1976)]. The possibilities for stabilization of ideal and resistive instabilities are explored systematically in different regions of parameter space. The study confirms that an ideal instability can be stabilized by a close-fitting wall and a rotation velocity on the order of resistive growth rates [J. Finn, Phys. Plasmas **2**, 3782 (1995)]. However, the region in parameter space where such stabilization occurs is very small and appears to be difficult to exploit in experiments. The overall conclusion from the cylindrical plasma model is that resistive modes can readily be wall stabilized, whereas complete wall stabilization is hard to achieve for plasmas that are ideally unstable with the wall at infinity.

PACS numbers: 52.30.Jb, 52.35.Py, 52.35.Dm, 52.55.Fa

[a]e-mail: elfab@elf.chalmers.se

I. Introduction

"Advanced tokamaks", where the main part of the plasma current comes from the bootstrap effect, require conducting walls to stabilize external kink modes at high beta.[1] Also, reversed field pinches need conducting walls for stabile operation.[2,3] In reality, a wall always has a finite conductivity, and this gives rise to another instability, the resistive wall mode, when the equilibrium is unstable in the absence of a wall.[4-8] The resistive wall mode grows on the resistive diffusion time of the wall, τ_w. Instability and locking of wall modes have been observed as precursors to disruption in wall stabilized tokamak discharges.[9] The resistive wall mode has rather different stability properties than modes stabilized by ideal walls. The stability of resistive wall modes has been discussed within both ideal and resistive magnetohydrodynamics (MHD) in several recent papers.[8,10,11,3,12] Here we apply the "resistive kink" dispersion relation,[13,14] that incorporates both resistive and ideal instabilities. It correctly includes the "damping" from coupling to the Alfvén continuum that was introduced in a somewhat *ad hoc* manner in Ref. 15. We establish conditions on the wall position and rotation frequency for the stabilization of MHD modes in different regions of parameter space.

It was shown in Ref. 8 that an ideal instability can be stabilized by a resistive wall, if the wall is sufficiently (but not too) far away from the plasma, and the plasma rotates with an ideal-MHD velocity, typically a few per cent of the Alfvén speed. Recently, Finn found that a cylindrical equilibrium that is ideally unstable with the wall at infinity can be stabilized by a close-fitting resistive wall and slow plasma rotation.[12] In the present study, we verify that this type of stabilization is possible in principle in cylindrical plasmas. However, the region in parameter space where such stabilization occurs is very small. This type of stabilization appears to be too fragile to be relevant to experiments, as it requires very precise control of both the resistive wall position and the plasma rotation frequency.

II. Formulation

We study resistive MHD instabilities in cylindrical equilibria with a single mode rational surface at $r = r_s$ where $q = m/n$ in the finitely conducting plasma. Sufficiently

far way from the rational surface, the perturbed magnetic flux ψ satisfies the static ideal MHD equation

$$\frac{1}{r}\frac{d}{dr}\left(r\frac{d\psi}{dr}\right) - \frac{m^2}{r^2}\psi - \left(\frac{mj'}{rF} + \frac{2m^2B_\theta{}^2p'}{B^2r^3F^2}\right)\psi = 0, \tag{1}$$

where $F = (B_\theta/r)(m - nq)$. The solutions of (1) will be matched by standard procedures at the resonant surface and joined to solutions in the vacuum region including a resistive shell. For the region outside the rational surface, we define two particular solutions for ψ: ψ_0 and ψ_∞, distinguished by their behavior in the vacuum.[3] ψ_0 is the solution of (1) with no wall, normalized so that $\psi_0 = 1$ at the radius of the resistive shell, $r = d$. The other solution ψ_∞ satisfies Eq. (1) for $r < d$, and has $\psi_\infty(d) = 0$ and $\psi'_\infty(d) = -1/d$. Thus, ψ_0 and ψ_∞ are solutions without a shell and with a perfectly conducting shell at the position of the resistive shell, respectively. (The subscripts correspond to the frequency for which the solution applies.) The actual solution of Eq. (1) for finite rotation frequency is a linear combination of ψ_0 and ψ_∞ for $r_s < r < d$.

Using the jump condition $\gamma\psi(d) = d[\psi'(d_+) - \psi'(d_-)]$, where γ is the growth rate, at the resistive shell, the jump in the logarithmic derivative of ψ at the rational surface can be expressed as[3]

$$\Delta' = \frac{\psi'(r_{s+}) - \psi'(r_{s-})}{\psi(r_s)} = \frac{\delta_0 + \gamma\tau_w\delta_\infty}{\psi_0 + \gamma\tau_w\psi_\infty}\ . \tag{2}$$

Here,

$$\delta_0 = \psi'_0(r_{s+}) - \psi'_0(r_{s-})\ ,\ \delta_\infty = \psi'_\infty(r_{s+}) - \psi'_\infty(r_{s-}) \tag{3}$$

denote the jumps in the radial derivative at the rational surface of the two basis solutions. For a given equilibrium, ψ_0, ψ_∞, δ_0 and δ_∞ can be calculated in terms of the plasma parameters and the wall position. In Appendix A, these quantities are calculated analytically for simple equilibrium profiles where the current density and pressure profiles are step functions. Depending on the current and pressure, the equilibria can be ideally or resistively unstable with the wall at infinity.

With an ideal wall, the stability properties depend on ψ_∞ and δ_∞ as follows:

- $\psi_\infty > 0, \delta_\infty < 0$, ideally and resistively stable,
- $\psi_\infty > 0, \delta_\infty > 0$, ideally stable, resistively unstable,

- $\psi_\infty < 0$, ideally unstable.

$\psi_0 = 0$ and $\psi_\infty = 0$ denote marginal stability of ideal kink modes for configurations without a wall, and with a perfectly conducting wall at $r = d$, respectively. Similarly, $\delta_0 = 0$ and $\delta_\infty = 0$ imply marginal stability of resistive modes without a wall, and with a perfectly conducting wall at $r = d$. Figure 1 is a schematic stability diagram in terms of normalized wall radius d/a versus normalized pressure $\hat{\beta}$. In region I the plasma is resistively unstable without a wall and resistively stable with an ideal wall. In regions II and III, the plasma is ideally unstable without a wall. In region II it resistively unstable and in region III resistively stable with an ideal wall.

At the resonant surface, we use the resistive kink dispersion relation,[13,14]

$$\hat{\Delta}_{in} = -\frac{\pi}{8}\hat{\lambda}^{5/4}\frac{\Gamma[\frac{1}{4}(\hat{\lambda}^{3/2}-1)]}{\Gamma[\frac{1}{4}(\hat{\lambda}^{3/2}+5)]}. \tag{4}$$

Here, $\hat{\Delta} \equiv \Delta' S^{-1/3}$ is the scaled Δ', $\hat{\lambda} \equiv \gamma\tau_A S^{1/3}$ the scaled growth rate, and S is the Lundquist number. This dispersion relation was derived by several authors.[13,14,16] Coppi et al[13,14] derived it under the restriction $\mathrm{Re}(\hat{\lambda}^{3/2}) > 1$, and Rosenau[16] later extended it to $\mathrm{Re}(\hat{\lambda}^{3/2}) > 0$. In Appendix B, we show that by proper analytical continuation in complex plane, the dispersion relation (4) holds for all $\hat{\lambda}$ with $|\arg(\hat{\lambda})| < \pi$. The zeroes of $\hat{\Delta}_{in}$ at $\hat{\lambda}^{3/2} = -5, -9, \ldots$ approximate the stable part of the resistive MHD spectrum.[17-20] The pole at $\hat{\lambda}^{3/2} = 1$ is associated with the resistive kink instability.[13,14]

We now assume that the plasma rotates with respect to the wall, so that there is a Doppler shift $\omega_0 = mv_\theta/r - nv_z/R$ at the rational surface. If $\hat{\lambda}$ denotes the scaled growth rate in the frame moving with the rational surface, the scaled external Δ' is

$$\hat{\Delta}_{ext} = \frac{\hat{\Delta}_0 + \alpha\hat{\Delta}_\infty(\hat{\lambda} - i\hat{\omega}_0)}{1 + \alpha(\hat{\lambda} - i\hat{\omega}_0)}, \tag{5}$$

where

$$\hat{\omega}_0 \equiv \omega_0\tau_A S^{1/3}, \quad \alpha \equiv S^{-1/3}\frac{\tau_w}{\tau_A}\frac{\psi_\infty}{\psi_0}, \quad \hat{\Delta}_0 \equiv S^{-1/3}\frac{\delta_0}{\psi_0}, \quad \hat{\Delta}_\infty \equiv S^{-1/3}\frac{\delta_\infty}{\psi_\infty}. \tag{6}$$

The eigenvalues are determined from the dispersion relation

$$\hat{\Delta}_{in}(\hat{\lambda}) = \hat{\Delta}_{ext}(\hat{\lambda}). \tag{7}$$

In the following, we analyze the solutions of the dispersion relation in the three regions indicated in Fig. 1.

III. Nyquist diagrams

The number of instabilities can be counted by means of the Cauchy principle. The dispersion relation (7) is written as $F(\hat{\lambda}) = \hat{\Delta}_{ext}(\hat{\lambda}) - \hat{\Delta}_{in}(\hat{\lambda})$. In regions where $F(\hat{\lambda})$ is analytic, the variation of $\arg[F(\hat{\lambda})]/2\pi$, as $\hat{\lambda}$ traverses a contour in the $\hat{\lambda}$-plane in the posistive sense, equals the number of zeroes minus the number of poles for $F(\hat{\lambda})$ inside the $\hat{\lambda}$-contour. We let $\hat{\lambda}$ traverse a contour consisting of a large semicircle $\hat{\lambda} = Re^{i\theta}$, $-\pi/2 < \theta < \pi/2$, $R \to \infty$, and the imaginary axis $\hat{\lambda} = i\hat{\omega}$ traversed from $\hat{\omega} = +R$ to $\hat{\omega} = -R$, with an infinitesimal indentation such that the origin is not encircled.

Figure 2 shows $C(i\hat{\omega}_0) = -\hat{\Delta}_{in}(i\hat{\omega})$, which forms a closed curve in the complex plane, while $\hat{\omega}$ varies from 0 to ∞. If we use the resistive approximation of the dispersion relation, the image $-\hat{\Delta}_{in}$ will take the form shown in Fig. 3. With the full dispersion relation, the $-\hat{\Delta}_{in}$ contour takes the form shown in Fig. 4. The full dispersion relation contains a pole for $\hat{\Delta}_{in}$ in the unstable halfplane, while the resistive approximation has no pole.

The image $\hat{\Delta}_{ext}(\hat{\lambda})$ is a circle that touches the real axis at $\hat{\Delta}_\infty$ for $\hat{\omega} \to \pm\infty$ and at $\hat{\Delta}_0$ for $\hat{\omega} = \hat{\omega}_0$. The $\hat{\Delta}_{ext}$ circle is traversed in the positive sense if $\psi_0\psi_\infty$(or α) is positive, and in the negative sense if $\psi_0\psi_\infty$ is negative, i.e., if the wall-at-infinity configuration is ideally unstable and the resistive wall is placed inside the ideal marginal wall position. $\hat{\Delta}_{ext}$ has one pole in the unstable half plane if $\psi_0\psi_\infty < 0$, otherwise no pole.

We now simplify matters by assuming that the wall time is much longer than typical resistive growth rates. This means that the $\hat{\Delta}_{ext}$ circle is traversed over a small frequency interval, during which the locus on the $\hat{\Delta}_{in}$ contour remains fixed. Then, the F contour can be constructed as the $-\hat{\Delta}_{in}$ contour shifted by $\hat{\Delta}_\infty$, with the $\hat{\Delta}_{ext}$ circle added onto it, at $\hat{\omega} = \hat{\omega}_0$. By this procedure, it is straightforward to analyse the number of instabilities and their nature.

A. Resistive instability with the wall at infinity

We first consider the case where the equilibrium is resistively unstable but ideally stable with the wall at infinity, i.e., $\psi_0 > 0$, $\delta_0 > 0$. To stabilize this case, it is necessary to place the wall in a position where an ideal wall would stabilize the resisitive tearing mode $\psi_\infty > 0$, $\delta_\infty < 0$, that is, in region I in Fig. 1. A Nyquist plot based on the resistive

dispersion relation shows that there is one instability if ω_0 is below some threshold value, and no instability if ω_0 exceeds the threshold. This represents the wall stabilization of resistive modes by slow rotation, as discussed by several authors.[5-7,11]

It is instructive to analyse the full dispersion relation for this case. The full dispersion relation has one pole, and the F curve encircles the origin 0 or 1 times in the positive sense. The naive interpretation is that there is either one or two instabilities. However, this conclusion is incorrect. In this case, a false root is created by the idealized behavior of $\hat{\Delta}_{in}(\hat{\lambda})$ at large $|\hat{\lambda}|$. It is well established that in the case of an ideal wall, there is a spurious root to $\Delta_{in}(\lambda) = \Delta_\infty < 0$, when $\delta_\infty < 0$ and $\psi_\infty > 0$. Greene and Miller[21] showed that the spurious root corresponds to $|\lambda|$ so large that the thin layer approximation breaks down. In the present application, the resonance with the Alfvén continuum (which occurs at the rational surface for zero rotation velocity and moves away from it with increasing rotation speed) would move from the mode rational surface into the vacuum. This extra root is not physical, and there is either 0 or 1 instability. On the other hand, the Nyquist diagram of the full dispersion relation does show that an "ideal" instability can be created if ω_0 is large enough.[10,12]

We conclude that, the resistively unstable case can be stabilized by a resistive wall in region I, if the rotation speed is larger than some resistive threshold, but less than an ideal critical speed.

B. Ideal instability with the wall at infinity

The equilibrium is ideally unstable without a wall if $\psi_0 < 0$, $\delta_0 > 0$. We first examine configurations where an ideal wall gives ideal stability but resistive instability, $\psi_\infty > 0$, $\delta_\infty > 0$, i.e., region II in Fig. 1. In this case, $\hat{\Delta}_{ext}$ has one pole in the unstable half-plane. The resistive dispersion relation shows that there is one instability at zero rotation frequency, and one additional instability appears when the rotation velocity exceeds a resistive threshold. It is appropriate to refer to the first as a tearing mode and the second as the resistive wall mode.

By considering the full dispersion relation we see that the resistive wall mode is stabilized if ω_0 exceeds an *ideal* threshold. Thus, an ideal instability can be stabilized by an

ideal rotation speed, as found in Ref. 8. However, there is a significant difference between the cylindrical and toroidal cases. In the low-beta cylindrical theory applied here, the *tearing* mode remains unstable for any rotation velocity. However, the toroidal numerical results[22] from the resistive MARS code,[23] showed that in a tokamak, the resistive stability boundary for resistive wall modes is close to the ideal stability boundary. The small influence of resistivity in a torus is quite expected, because resistive MHD modes are stabilized by favorable averaged curvature in toroidal equilibria with $q > 1$.[24]

The final case to discuss is when the wall position is close enough so that an ideal wall makes the plasma resistively stable, $\psi_\infty > 0$, $\delta_\infty < 0$ (region III in Fig. 1). A Nyquist plot based on the resistive approximation now reveals that there is one instability if $\omega_0 = 0$ (one pole in $\hat{\Delta}_{ext}$ and the origin is not encircled). If the ratio Δ_0'/Δ_∞' is sufficiently small, or sufficiently large, there is a small window of frequencies in the resistive range, where the origin is encircled once in the negative sense, and there is no instability. This confirms the result of Finn.[12] However, as will be shown in Sect. IV, this stable region is very small.

If we use the complete dispersion relation, the number of times the origin is encircled does not change, but there is one more pole in $\hat{\Delta}_{in}$. Therefore, the complete dispersion relation appears to predict another instability. However, for the same reason as discussed in Sect. III.A, this is a spurious ideal mode that appears when $\delta_\infty < 0$ and $\psi_\infty > 0$.

Consequently, in region III, there is either one or no instability. The instability can be referred to as a resistive wall mode. If Δ_0'/Δ_∞' is sufficiently large, or sufficiently small, the resistive wall mode can be stabilized by rotation frequencies in a small window of tearing growth rates.

IV. Analysis

A. Different limits of the dispersion relation

Various instabilities can be recovered from the dispersion relation (7) in different limits: $|\hat{\lambda}| \gg 1$, ideal kinks, $\hat{\lambda} \simeq 1$, resistive kinks, and $|\hat{\lambda}| \ll 1$, tearing modes. In the high frequency limit where the plasma behaves ideally ($|\hat{\lambda}| >> 1$), so that $\Delta_{in} \approx -\pi/\hat{\lambda}$,

Eq. (7) becomes a quadratic equation for $\hat{\lambda}$.[3] This will be referred to as the "ideal" dispersion relation. In the tearing limit, $|\hat{\lambda}| \ll 1$, we set $\hat{\lambda} = 0$ in the gamma functions. This gives

$$\hat{\Delta}_{in} = \frac{\hat{\lambda}^{5/4}}{h}, \quad h = \frac{1}{2\pi}\frac{\Gamma(\frac{1}{4})}{\Gamma(\frac{3}{4})} \simeq 0.4709. \tag{8}$$

The resistive-plasma-resistive-wall dispersion relation was analyzed in Ref. 7.

The resistive kink pole of $\hat{\Delta}_{in}$ of implies that $\hat{\Delta}_\infty \to \infty$ as $\hat{\lambda} \to 1$, which means marginal stability to ideal MHD modes. To see the effects of a resistive wall on the resistive kink, we expand the right hand side of (4) around $\hat{\lambda} = 1$ and obtain $\hat{\Delta}_{in} \simeq -\frac{2}{3}\pi^{1/2}/(\hat{\lambda}-1)$. Assuming $|\alpha| \gg 1$ (i.e., $\tau_w \gg \tau_A S^{1/3}$), one can approximate the growth rate for resistive kink mode,

$$\hat{\lambda} \simeq 1 - \frac{2}{3}\pi^{1/2}\frac{1}{\hat{\Delta}_\infty}\left[1 + \frac{\hat{\Delta}_\infty - \hat{\Delta}_0}{\alpha(1 - i\hat{\omega}_0)\hat{\Delta}_\infty}\right]. \tag{9}$$

In terms of physical quantities, this gives

$$\gamma\tau_A = S^{-1/3} - \frac{2}{3}\pi^{1/2}\left[\frac{1}{\Delta'_\infty} + \frac{\psi_0}{\delta_\infty}\left(1 - \frac{\Delta'_0}{\Delta'_\infty}\right)\frac{\tau_A/\tau_w}{S^{-1/3} - i\omega_0\tau_A}\right]. \tag{10}$$

At the marginal point of the ideal mode, $\psi_\infty = 0$, the resistive kink is unstable with a growth rate that scales as $S^{-1/3}$. For a perfectly conducting wall, $\tau_w/\tau_A \to \infty$, and (10) reduces to the result found by Ara, *et al.*[14]

Equation (10) shows that if τ_w is large compared with $\tau_A S^{1/3}$, the contribution from the resistive wall and plasma rotation is small in the region where Eq. (10) holds, i.e., $\Delta'_\infty = O(S^{1/3})$. In this region, the growth rate is not much affected by the resistivity of the wall and the plasma rotation. For the resistive kink case, we have $\psi_0 < 0$ and $\delta_\infty > 0$, and Eq. (10) shows that rotation slightly decreases the growth rate.

B. The resistive wall mode

It is particularly instructive to consider the limit of large wall time. Generally, the wall mode has $\lambda = i\omega_0 + O(1/\tau_w)$. When the wall time is much longer than the growth time of the tearing mode, we can set $\hat{\lambda} \approx i\hat{\omega}_0$ in the internal Δ' [Eq. (4)]. The expression for the external Δ' [Eq. (5)] then gives $\hat{\lambda}$ as an explicit function of $\hat{\omega}_0$:

$$\hat{\lambda} = i\hat{\omega}_0 - \frac{1}{\alpha}\frac{\hat{\Delta}_0 + C}{\hat{\Delta}_\infty + C}, \tag{11}$$

where

$$C(i\hat{\omega}_0) \equiv -\hat{\Delta}_{in}(i\hat{\omega}_0) = (i\hat{\omega}_0)^{5/4}\frac{\pi}{8}\frac{\Gamma\{\frac{1}{4}[(i\hat{\omega}_0)^{3/2}-1]\}}{\Gamma\{\frac{1}{4}[(i\hat{\omega}_0)^{3/2}+5]\}}. \tag{12}$$

Figure 2 shows $C(i\hat{\omega}_0)$, which forms a closed curve in the complex plane, when $\hat{\omega}_0$ varies from 0 to ∞. The arrow indicates the direction of increasing $\hat{\omega}_0$.

When the rotation frequency is much larger than the resistive kink growth rate, $\hat{\omega}_0 \equiv \omega_0\tau_A S^{1/3} \gg 1$, the ideal approximation applies and $C = -i\pi/\hat{\omega}_0$. When $\hat{\omega}_0 \ll 1$, (but still ω_0 is much faster than the tearing growth rate so that the approximation $\lambda \approx i\omega_0$ holds), the tearing approximation applies, and $C(i\hat{\omega}_0) = -(i\hat{\omega}_0)^{5/4}/h$. The regimes where the ideal and tearing approximations hold are the two straight sections of the $C(i\hat{\omega}_0)$ curve approaching the origin in Fig. 2.

Marginal stability is found by letting $\mathrm{Re}(\hat{\lambda}) = 0$ in (11), which gives

$$|C|^2 + \left(\hat{\Delta}_0 + \hat{\Delta}_\infty\right)\mathrm{Re}(C) + \hat{\Delta}_0\hat{\Delta}_\infty = 0. \tag{13}$$

This represents a circle in the complex plane through $C = -\hat{\Delta}_0$ and $C = -\hat{\Delta}_\infty$. It is the contour $C = -\hat{\Delta}_{ext}(i\hat{\omega}), -\infty < \hat{\omega} < \infty$.

1. Region II: Ideal instability with the wall at infinity and resistive instability with an ideal wall

Figure 5 shows the $C(i\hat{\omega}_0)$ curve together with the marginal stability circles, $\mathrm{Re}(\hat{\lambda}) = 0$ [Eq. (13)], for several different wall positions in a case where the wall-at-infinity configuration is ideally unstable ($\psi_0 < 0, \delta_0 > 0$). This specific case has $m = 2$, $n = 1$, $q_0 = 1$, $q_a = 2.3$, $\beta = 0.43$, $S = 10^6$. When the wall time is long, the crossings of the $C = -\hat{\Delta}_{in}(i\hat{\omega}_0)$ curve and the circles give the marginal points for the wall mode. As discussed in Sect. III.B, the resistive wall mode is stable in region II ($1.049 < d/a < 1.254$ in Fig. 5) when $\hat{\omega}_0$ is either below some tearing value $\hat{\omega}_R$ or above some ideal value $\hat{\omega}_I$. In Fig. 5, the wall mode is stable when the point on the $-\hat{\Delta}_{in}(i\hat{\omega}_0)$ curve is located inside the circles (13). Thus, the resistive wall mode is unstable in a frequency window

$$\hat{\omega}_R < \hat{\omega}_0 < \hat{\omega}_I. \tag{14}$$

Outside this window, the wall mode is stable. In addition to the wall mode, there is an unstable tearing mode in the entire region II, as discussed in Sect. III.B.

The ideal marginal frequency $\hat{\omega}_I$ can be calculated as follows. For $\hat{\omega}_0 \gg 1$, we combine the ideal approximation for C and (13), to obtain $\hat{\omega}_I = \pi(-\hat{\Delta}_0\hat{\Delta}_\infty)^{-1/2}$, or in terms of physical quantities,

$$\omega_I \tau_A = \pi(-\Delta_0'\Delta_\infty')^{-1/2} . \tag{15}$$

This shows that ω_I is an ideal MHD frequency, independent of S. The required rotation frequency approaches zero at the top boundary of region II (the ideal stability limit, $\Delta_\infty' \to +\infty$) and infinity as the wall position approaches the boundary between regions II and III (the resistive stability boundary, $\Delta_\infty' \to 0^+$). Thus, the stability of the wall mode improves as the wall moves outward in region II, as found in Ref. 8.

For $\hat{\omega}_0 \ll 1$, we use the resistive approximation of the dispersion relation together with (13) and obtain the resistive bound on $\hat{\omega}_0$, below which the resistive wall mode is stable in region II:

$$\hat{\omega}_R^{5/4}/h = -\frac{1}{2}\left(\hat{\Delta}_0 + \hat{\Delta}_\infty\right)\sin\frac{\pi}{8} + \left[(\hat{\Delta}_0 + \hat{\Delta}_\infty)^2\frac{1}{4}\sin^2\frac{\pi}{8} - \hat{\Delta}_0\hat{\Delta}_\infty\right]^{1/2} \tag{16}$$

Equation (16) can expressed as

$$\omega_R \tau_A = S^{-3/5}(-h\Delta_0')^{4/5} f(\Delta_\infty'/\Delta_0'). \tag{17}$$

where f is a monotone function tending to $(\sin\pi/8)^{4/5}$ when $\Delta_\infty' \to 0^+$ (boundary between regions II and III) and to $(\sin\pi/8)^{-4/5}$ when $\Delta_\infty' \to +\infty$ (upper boundary of region II).

2. Region III: Ideal instability with the wall at infinity and resistive stability with an ideal wall

When the wall is moved inward from region II and reaches the tearing stability boundary (between regions II and III), the upper limiting frequency for the unstable window approaches infinity. In Fig. 5, this corresponds to the circle for $d/a = 1.049$. The infinite frequency, of course, brings the dispersion realtion outside its region of validity. The intersection of the $\mathrm{Re}(\hat{\lambda}) = 0$ circles with the ideal branch of the $C(i\hat{\omega}_0)$ curve moves over to the resistive branch at $C = 0$. At this switch-over, the other marginal point evolves continuously. The switch-over occurs when the wall radius enters region III, where there is a small, completely stable window, as discussed in Sect. III.B. For this complete stabilization, ω_0 must be between two limits, that are both of the order of a resistive growth

rate. The frequency limits are given by [cf. (16)]

$$\hat{\omega}_{R\pm}^{5/4}/h = -\frac{1}{2}\left(\hat{\Delta}_0 + \hat{\Delta}_\infty\right)\sin\frac{\pi}{8} \pm \left[(\hat{\Delta}_0 + \hat{\Delta}_\infty)^2\frac{1}{4}\sin^2\frac{\pi}{8} - \hat{\Delta}_0\hat{\Delta}_\infty\right]^{1/2} \tag{18}$$

In region III, both Δ_0' and Δ_∞' are positive, and in order for the frequencies (18) to be real, Δ_0'/Δ_∞' has to be sufficiently large or sufficiently small. Equation (18) shows that stabilization is not possible when

$$\frac{1}{g} < \Delta_\infty'/\Delta_0' < g\ , \quad g = \left(\frac{1+\cos\pi/8}{\sin\pi/8}\right)^2 \simeq 25.3 \tag{19}$$

Thus, the condition for complete stability in region III is very restrictive. The condition is satisfied near the boundary to region II, where Δ_∞'/Δ_0' is small. Further into region II, $|\Delta_\infty'|$ increases and stabilization is lost (for $d/a < 1.035$ in Fig. 5). In addition, the rotation frequency is restricted to a window in the range of resistive growth rates. For reversed field pinches, such restrictive conditions would typically have to be satisfied for several different toroidal mode numbers, and the different conditions may well be in conflict with one another. We conclude that this type of stabilization is difficult to achieve in practice. The complete stabilization in region III is also very sensitive to the nature of the dispersion relation. For instance, for the viscous tearing mode, where $\Delta_{in}' \propto \gamma$,[25] complete stabilization is not possible in region III.

3. Region I: Resistive instability with the wall at infinity, resistive stability with an ideal wall

In region I, the picture is simple. From the Nyquist diagrams discussed in Sect. III.A, we understand that the wall mode is *stable* in a window of the rotation frequency, $\omega_R < \omega_0 < \omega_I$, where ω_I and ω_R are given by (15) and (16), respectively. The stable window shrinks as the wall is moved closer to the plasma. The limiting expressions are now $\omega_R\tau_A = S^{-3/5}(-h\Delta_\infty'/\sin\pi/8)^{4/5}$ as $\Delta_\infty \to 0^-$ (upper boundary of region I) and $\omega_R\tau_A = S^{-3/5}(-h\Delta_\infty'\sin\pi/8)^{4/5}$ as $\Delta_\infty \to -\infty$.

C. Summary of analytic results

For the analysis, we have so far assumed that the wall time is long compared with other time scales. Modifications resulting from finite wall time are discussed in Appendix C.

Finite wall time changes the critical rotation frequencies but not the qualitative aspects of the results in regions I, II and III. We can therefore draw the following conclusions.

When the equilibrium is resistively unstable with the wall at infinity, and the ideal wall configuration is resistively stable ($\delta_\infty < 0$, region I), there is a completely stable window for the rotation frequency. The Doppler shift should be greater than a certain resistive value (16) [with finite wall time (C8)] but slower than an ideal frequency (15) [with finite wall time (C4)].

For configurations that are ideally unstable with the wall at infinity ($\psi_0 < 0$) but ideally stable with a perfectly conducting wall ($\psi_\infty > 0$), the following holds:

1. The tearing mode remains unstable as long as $\delta_\infty > 0$, i.e., in the entire region II.

2. The resistive wall mode can be stabilized in region II (the ideal-wall configuration resistively unstable) either by rotating the plasma above an ideal threshold frequency, or below a threshold frequency of the order of tearing growth rates.

3. The required ideal rotation frequency in region II decreases with increasing wall distance. It approaches infinity when $\Delta_\infty \to 0^+$, i.e., when the resistive-wall configuration is resistively stabilized by a perfectly conducting wall.

4. When the wall moves closer to the plasma so that the tearing mode is stabilized ($\delta_\infty < 0$, region III), a completely stable, but very narrow, window in frequency exists if the ratio Δ_0'/Δ_∞' is sufficiently different from unity [Eq. (19)]. As this window is very narrow, we do not believe it has any experimental significance.

V. Conclusions

We have examined the stabilization of cylindrical plasmas by resistive walls and plasma rotation by applying the resistive kink dispersion relation. Various ways of stabilization have been investigated and the relation of different instabilities has been clarified.

The stability properties with an ideal wall indicated in Fig. 1 determine the possibilities for stabilization with a resistive wall and plasma rotation. In region I, the plasma is resistively unstable without a wall and resistively stable with an ideal wall. Then, the

plasma can be completely stabilized by a resistive wall and rotation by a frequency above a tearing growth rate[5–7,11,3] (C8). In this region, rotation above an ideal threshold (15) will destabilize the resistive wall mode.[10,12]

In region II, the plasma is ideally unstable without a wall and resistively unstable with an ideal wall. The resistive wall mode is then stabilized by rotating the plasma above an ideal threshold[8,22,3] (15). Furthermore, that the resistive wall mode is stable when the rotation frequency is below some resistive tearing growth rate (C8). However, in the whole of region II, the resistive tearing mode is unstable, independent of the rotation frequency.

Finally, in region III, the plasma is ideally unstable without the wall, but resistively stable with an ideal wall. In this region, a mode of resistive wall nature is typically unstable. However, there is a window of *complete stability* near the boundary between regions II and III, cf. Eq. (19), and the rotation speed is in the range of resistive tearing growth rates (18).[12] This region of complete stability is very small, and most likely does not have any experimental significance.

The overall conclusion from the adopted cylindrical model therefore becomes as follows. Equilibria that are resistively unstable in the absence of a wall can be stabilized by a slow rotation provided the resistive wall is inside the marginal position of an ideal wall for resistive modes. Equilibria that are ideally unstable in the absence of a wall can be made ideally stable by an ideal rotation velocity if the resistive wall is inside the ideal marginal position. However, when the wall-at-infinity configuration is ideally unstable, it is very difficult to wall stabilize resistive modes. This last conclusion on resistive stability in cylindrical geometry is more pessimistic than the numerical resistive MHD results for toroidal external kinks in tokamaks.[22] The resistive stability in toroidal geometry is very likely connected with favorable curvature.[24]

References

[1]C. Kessel, J. Manickam, G. Rewoldt, and W. M. Tang, Phys. Rev. Lett. **72**, 1212 (1994).

[2]D. C. Robinson, Nucl. Fusion **18**, 939 (1978).

[3]X. Z. Jiang, A. Bondeson and R. Paccagnella, Phys. Plasmas **2**, 442 (1995).

[4]D. Pfirsch and H. Tasso, Nucl. Fusion **11**, 259 (1971).

[5]T. H. Jensen and M. S. Chu, J. Plasma Phys. **30**, 57 (1983).

[6]C. G. Gimblett, Nucl. Fusion **26**, 617 (1986).

[7]A. Bondeson and M. Persson, Nucl. Fusion **28**, 1887 (1988).

[8]A. Bondeson and D. J. Ward, Phys. Rev. Lett. **72**, 2709 (1994).

[9]E. J. Strait, T. S. Taylor, A. D. Turnbull, J. R. Ferron, L. L. Lao, B. Rice, O. Sauter, S. J. Thompson, and D. Wróblewski, Phys. Rev. Lett. **74**, 2483 (1995).

[10]R. Betti and J. P. Freidberg, Phys. Rev. Lett. **74**, 2949 (1995).

[11]J. M. Finn, Phys. Plasmas **2**, 198 (1995).

[12]J. M. Finn, Phys. Plasmas **2**, 3782 (1995).

[13]B. Coppi, R. Galvão, R. Pellat, M. Rosenbluth, and P. Rutherford, Sov. J. Plasma Phys. **2**, 533 (1976) [Fiz. Plasmy **2**, 961 (1976)].

[14]G. Ara, B. Basu, B. Coppi, G. Laval, M. N. Rosenbluth, and B. V. Waddell, Annals Phys. **112**, 443 (1978).

[15]M. S. Chu, J. M. Greene, T. H. Jensen, R. L. Miller, A. Bondeson, R. W. Johnson, and M. E. Mauel, Phys. Plasmas **2**, 2236 (1995).

[16]P. Rosenau, Phys. Fluids **26**, 2578 (1983).

[17]C. M. Ryu and R. C. Grimm, J. Plasma Phys. **32**, 207 (1984).

[18]R. Dewar and B. Davis, J. Plasma Phys. **32**, 443 (1984).

[19]D. Lortz and G. Spies, in *Plasma Physics and Controlled Nuclear Fusion Research 1984*, Proceedings 10th International Conference, London, 1984 (IAEA, Vienna, 1985), Vol. 2, p. 245.

[20]W. Kerner, K. Lerbinger and K. Riedel, Phys. Fluids **29**, 2975 (1986).

[21]J. M. Greene, and R. Miller, Phys. Plasmas **2**, 1236 (1995).

[22]D. J. Ward and A. Bondeson, Phys. Plasmas **2**, 1570 (1995).

[23]A. Bondeson, G. Vlad, and H. Lütjens, Phys. Fluids **B4**, 1899 (1992).

[24]A. H. Glasser, J. M. Greene, and J. L. Johnson, Phys. Fluids **18**, 875 (1975).

[25]A. Bondeson and J. Sobel, Phys. Fluids **27**, 2028 (1984).

[26]A. Erdélyi, W. Magnus, F. Oberhettinger, and F. G. Tricomi, *Higher Transcendental Functions* (McGraw-Hill, New York, 1953), Vol I, Sect. 1.6.

Appendix A. External solutions for a model equilibrium

Away from resonant surface r_s, the perturbed flux function satisfies the external equation (1). We consider a family of equilibria, for which the external solution can be found analytically, similar to the equilibria treated by Finn.[12] We let $j(r)$ be a step function, $j = j_0 = 2B/Rq_0 = 2B_\theta/r$ inside a certain radius $r < r_0$, and $j = 0$ for $r > r_0$. The pressure is assumed constant across the plasma and falls to zero at the plasma-vacuum boundary $r = a$. Inside the resonant surface, Eq. (1) gives

$$\left(\frac{\psi'}{\psi}\right)_{r=r_s^-} = \frac{m}{r_s}\,\frac{m - nq_0 - 1 - (nq_0/m)^m}{m - nq_0 - 1 + (nq_0/m)^m} \equiv D_i. \tag{A1}$$

For the region outside the resonant surface, ψ_0 is defined as the solution in the absence of a wall, normalized to 1 at the location of the resistive wall, $r = d$. This gives

$$\psi_0(r_s^+) = \left(\frac{d}{a}\right)^m \left[(1-\hat\beta)\left(\frac{a}{r_s}\right)^m + \hat\beta\left(\frac{r_s}{a}\right)^m\right],$$

$$\psi_0'(r_s) = \frac{m}{r_s}\left(\frac{d}{a}\right)^m \left[\hat\beta\left(\frac{r_s}{a}\right)^m - (1-\hat\beta)\left(\frac{a}{r_s}\right)^m\right],$$

where

$$\hat\beta = \frac{\beta}{2}\frac{m}{(m-nq_a)^2} \tag{A2}$$

ψ_∞ is defined as the solution for $r < d$ such that $\psi_\infty = 0$ and $\psi_\infty' = -1/d$. This gives

$$\psi_\infty(r_s) = \frac{1}{2m}\left[\left(\frac{d}{a}\right)^m\left(1-\hat\beta\right) + \hat\beta\left(\frac{a}{d}\right)^m\right]\left(\frac{a}{r_s}\right)^m + \frac{1}{2m}\left[\left(\frac{d}{a}\right)^m\hat\beta - \left(1+\hat\beta\right)\left(\frac{a}{d}\right)^m\right]\left(\frac{r_s}{a}\right)^m$$

$$\psi_\infty'(r_s^+) = \frac{-1}{2r_s}\left[\left(\frac{d}{a}\right)^m\left(1-\hat\beta\right) + \hat\beta\left(\frac{a}{d}\right)^m\right]\left(\frac{a}{r_s}\right)^m + \frac{1}{2r_s}\left[\left(\frac{d}{a}\right)^m\hat\beta - \left(1+\hat\beta\right)\left(\frac{a}{d}\right)^m\right]\left(\frac{r_s}{a}\right)^m$$

The quantities δ_0 and δ_∞ are defined as the jumps in the radial derivative of ψ at the resonant surface, i.e.,

$$\delta_0 = \psi_0'(r_s^+) - \psi_0(r_s)D_i\ ,\quad \delta_\infty = \psi_\infty'(r_s^+) - \psi_\infty(r_s)D_i\ .$$

Appendix B. Inner layer solution for arbitrary λ

Here, we show how the resistive kink dispersion relation, derived by Coppi *et al.*[13,14] for $\mathrm{Re}(\hat\lambda)^{3/2} > 1$, can be extended to arbitrary $\hat\lambda$. The equations describing the dynamics

of the plasma within the inner layer can be written as[14,16]

$$\lambda^2 d^2\xi/d^2x = x d^2\psi/dx^2 \tag{B1}$$

$$(\epsilon/\lambda) d^2\psi/dx^2 - x\xi = \psi \ . \tag{B2}$$

Here $x \equiv (r - r_s)/r_s$, ξ is the radial displacement, and $\psi \equiv ib_r/(r_s F')$, where b_r is the radial component of the perturbed magnetic field. The normalized growth rate is $\lambda \equiv \gamma\tau_A$ and $\epsilon \equiv 1/S$ is a normalized resistivity. By introducing

$$\chi(x) = x d\psi/dx - \psi = \lambda^2 d\xi/dx + \chi_\infty,$$

where χ_∞ is a constant determined by matching to outer layer solution, Eqs. (B1) and (B2) are reduced to

$$\epsilon\lambda\left(\frac{d^2\chi}{dx^2} - \frac{2}{x}\frac{d\chi}{dx}\right) - \left(x^2 + \lambda^2\right)\chi = -x^2\chi_\infty. \tag{B3}$$

Matching to the outer layer solution requires

$$\chi_\infty = \frac{2}{\pi}\lambda_h \int_0^\infty \frac{1}{x}\frac{d\chi}{dx} dx \tag{B4}$$

where $\lambda_h = -\pi/\Delta'$.

We transform (B3) by setting $s = x^2(\epsilon\lambda)^{-1/2}$ [where $|\arg(\hat{\lambda})| < \pi$ is assumed], $\sigma = \hat{\lambda}^{3/2} = \lambda^{3/2}\epsilon^{-1/2}$, and $\chi/\chi_\infty = 1 + Z$, which results in

$$sZ'' - \frac{1}{2}Z' - \frac{1}{4}(s + \sigma)Z = \frac{\sigma}{4} \ . \tag{B5}$$

The solution $Z(s)$ must approach 0 as $s \to +\infty$ and its series expansion around $s = 0$ must not contain half-integer powers. A Fourier transformation

$$Z(s) = \frac{1}{2\pi}\int e^{iks} Z(k) dk, \tag{B6}$$

where the integration contour is yet to be determined, turns (B5) into a first-order equation in k

$$\frac{d}{dk}\left[\left(k^2 + \frac{1}{4}\right)Z\right] + \left(\frac{k}{2} - \frac{i\sigma}{4}\right)Z = \frac{i\pi\sigma}{2}\delta(k). \tag{B7}$$

To solve this, we set

$$Y = \left(k^2 + \frac{1}{4}\right)Z$$

which gives

$$\frac{dY}{dk} + \frac{1}{4}\left(\frac{1+\sigma}{k+i/2} + \frac{1-\sigma}{k-i/2}\right) Y = \frac{i\sigma\pi}{2}\delta(k) \ .$$

A solution for k real and positive is:

$$Y(k) = \frac{i\sigma\pi}{2}(1-2ik)^{-(1+\sigma)/4}(1+2ik)^{-(1-\sigma)/4} \ .$$

The Fourier transform therefore becomes

$$Z(k) = 2\pi i\sigma(1-2ik)^{-(5+\sigma)/4}(1+2ik)^{-(5-\sigma)/4} \ .$$

To find an appropriate integration contour for Eq. (B6), we first change the variable of integration from k to $t = -2ik$ and obtain

$$Z(s) = -\frac{\sigma}{2}\int_\Gamma G(t)\exp(-st/2)dt \ , \quad G(t) = (1+t)^{-(5+\sigma)/4}(1-t)^{-(5-\sigma)/4} \tag{B8}$$

We substitute (B8) into (B5) and find that the equation is satisfied if the contributions from the endpoints of the integration contour Γ, say t_+ and t_-, satisfy the condition

$$G(t_+)\exp(-st_+/2) - G(t_-)\exp(-st_-/2) = -1 \tag{B9}$$

for all $s > 0$. In the case discussed by Coppi *et al.*,[13,14] $\mathrm{Re}(\sigma) > 1$, it is sufficient to take $t_- = 0$ and $t_+ = 1$ because the endpoint contribution vanishes at $t = 1$. When $\mathrm{Re}(\sigma) < 1$, this prescription does not work because the contribution from $t = 1$ diverges.

This problem is solved by modifying the integration contour. We place the cut of the integrand along the real t-axis. The integration contour starts at $t_- = i0^-$, where we define $\arg(1-t_-) = 0$. The integration contour then encircles the branch point at $t = 1$ in the positive (counter-clockwise) sense and returns to $t_+ = i0^+$, where $\arg(1-t_+) = 2\pi$. To compensate for the changed integration contour, we must renormalize $G(t)$ so that (B9) holds. Using the notation of Ref. 26 for the integration contour, the solution can be written as

$$\frac{\chi}{\chi_\infty} = 1 - \frac{\sigma/2}{1-\exp[i\pi(\sigma-5)/2]}\int_0^{(1+)}(1+t)^{-(5+\sigma)/4}(1-t)^{-(5-\sigma)/4}\exp(-st/2)dt \tag{B10}$$

This is to be substituted in the matching condition (B4) where the integration over x becomes trivial. In the remaining integral over t, we set $t = (1-y)/(1+y)$, and obtain

$$\frac{\epsilon^{1/3}}{\lambda_h} = \frac{\hat{\lambda}^{5/4}}{4\pi^{1/2}}\frac{1}{\exp[i\pi(\sigma-5)/2]-1}\int_1^{(0+)} y^{(\sigma-5)/4}(1-y)^{1/2}dy$$

$$= \frac{\hat{\lambda}^{5/4}}{4\pi^{1/2}} B\left(\frac{1}{4}(\hat{\lambda}^{3/2}-1), \frac{3}{2}\right) , \tag{B11}$$

where $B(u,v) = \Gamma(u)\Gamma(v)/\Gamma(u+v)$ is the beta function.[26] Equation (B11) gives the dispersion relation

$$\hat{\Delta}_{in} = -\frac{\pi}{8}\hat{\lambda}^{5/4}\frac{\Gamma[\frac{1}{4}(\hat{\lambda}^{3/2}-1)]}{\Gamma[\frac{1}{4}(\hat{\lambda}^{3/2}+5)]}. \tag{B12}$$

for arbitrary $\hat{\lambda}$ with $|\arg(\hat{\lambda})| < \pi$. We note that along the rays $\arg(\hat{\lambda}) = \pm 2\pi/3$, $\hat{\lambda}$ has poles at $\hat{\lambda} = (4n-1)^{2/3}\exp(\pm 2\pi i/3)$ and zeroes at $\hat{\lambda} = (4n+1)^{2/3}\exp(\pm 2\pi i/3)$, for $n = 1, 2\ldots$. Thus for any $\hat{\Delta}$, there are sequences of solutions along these rays in the stable part of the λ-plane.[17,19,20] Since $\hat{\Delta} = \Delta' S^{-1/3} \to 0$ as $S \to \infty$, the eigenvalues at large S lie close to the zeroes of $\hat{\Delta}$ at

$$\hat{\lambda} = 0 , \quad \hat{\lambda} = (4n+1)^{2/3}\exp(\pm 2\pi i/3) , \quad n = 1, 2, \ldots \tag{B13}$$

Appendix C. Influence of finite wall time

For a finite wall time τ_w, the picture is similar to that discussed section IV.B, but the marginal rotation frequencies are modified. Here, we discuss the modifications analytically in the limits of the tearing and ideal dispersion relations, following essentially the treatment in Ref. 3. Letting $\hat{\lambda} = i\hat{\omega}$, purely imaginary, in the ideal or tearing limits of the dispersion relation we obtain conditions that determine the mode frequency $\hat{\omega}$ at the marginal point.

At large $\hat{\omega}_0$, we can use the ideal approximation. Using the phase information of the dispersion relation

$$\frac{\hat{\Delta}_0 + i\alpha\hat{\Delta}_\infty(\hat{\omega}-\hat{\omega}_0)}{1+i\alpha(\hat{\omega}-\hat{\omega}_0)} = \frac{i\pi}{\hat{\omega}} \tag{C1}$$

we find for $u = \alpha(\hat{\omega}_0 - \hat{\omega})$

$$u = (-\Delta_0/\Delta_\infty)^{1/2}\mathrm{sgn}(\alpha). \tag{C2}$$

The minimum Doppler shift needed for stabilization is then obtained as

$$\hat{\omega}_I = \left|\frac{u}{\alpha}\right| + \pi(-\hat{\Delta}_0\hat{\Delta}_\infty)^{-1/2}. \tag{C3}$$

In terms of physical quantities,

$$\omega_I = \frac{1}{\tau_w}\left(-\frac{\psi_0\delta_0}{\psi_\infty\delta_\infty}\right)^{1/2} + \frac{\pi}{\tau_A}(-\Delta_0'\Delta_\infty')^{-1/2}. \tag{C4}$$

The first term in (C4) represents the rotation of the mode with respect to the wall, and is of the order of inverse wall time. The second term represents the slippage of the mode relative to the plasma at the resonant surface, and is comparable to an ideal growth rate. As generally $\tau_w \gg \tau_A$, the second term is dominant.

When the rotation frequency is comparable to tearing growth rates, the dispersion relation can be approximated as:

$$\frac{\hat{\Delta}_0 + i\alpha\hat{\Delta}_\infty(\hat{\omega} - \hat{\omega}_0)}{1 + i\alpha(\hat{\omega} - \hat{\omega}_0)} = \frac{(i\hat{\omega})^{5/4}}{h} \tag{C5}$$

In the same way as above, we obtain the Doppler shift needed for stabilization,

$$\hat{\omega}_R = \left|\frac{u}{\alpha}\right| + h^{4/5}\left(\frac{\hat{\Delta}_0^2 + u^2\hat{\Delta}_\infty^2}{1+u^2}\right)^{2/5}, \tag{C6}$$

where u satisfies

$$u^2 + \tan\frac{\pi}{8}\left(\frac{\Delta_0}{\Delta_\infty} - 1\right)u + \frac{\Delta_0}{\Delta_\infty} = 0, \tag{C7}$$

and the root must be chosen so that $u\alpha > 0$. [Note that the discriminant in (C7) is simply related to that for $|C|$ in (13) so that the condition on Δ_0'/Δ_∞' for real solutions is the same.] When $\Delta_0/\Delta_\infty < 0$, $|u|$ varies from ∞ when $\Delta_\infty \to 0$ to 0 when $|\Delta_\infty| \to \infty$. The second term in Eq. (C6) is a more compact way of writing the slip frequency between the mode and the plasma, Eq. (16). The marginal frequencies can be expressed in terms of physical quantities as

$$\omega_R = \left|\frac{u\psi_0}{\tau_w\psi_\infty}\right| + h^{4/5}\left(\frac{\Delta_0^2 + u^2\Delta_\infty^2}{1+u^2}\right)^{2/5}\frac{S^{-3/5}}{\tau_A} \tag{C8}$$

Figures

FIG. 1. Schematic stability diagram showing the different regions of stability in terms of normalized wall distance d/a and normalized pressure $\hat{\beta}$.

FIG. 2. Contour $C = -\hat{\Delta}_{in}(i\hat{\omega})$ in the complex plane, for $\hat{\omega}$ varying from 0 to ∞. The arrow indicates the direction of increasing $\hat{\omega}$.

FIG. 3. (a) Nyquist contour in $\hat{\lambda}$-plane and (b) image contour $-\hat{\Delta}_{in}(\hat{\lambda})$ for the resistive approximation.

FIG. 4. (a) Nyquist contour in $\hat{\lambda}$-plane and (b) image contour $-\hat{\Delta}_{in}(\hat{\lambda})$ for the full dispersion relation (4).

FIG. 5. Complex C, or $-\hat{\Delta}$-plane for $m = 2$, $n = 1$ and the model equilibrium with $q_0 = 1$, $q_a = 2.3$, $\beta = 0.43$, $S = 10^6$ (ideally unstable with the wall at infinity). The solid line is the $-\hat{\Delta}(i\hat{\omega})$ contour shown in Fig. 2. The dotted circles correspond to marginal stability from the external solution including the resistive wall at radii d/a marked in the figure. For an ideal wall the marginal position is $d/a = 1.049$ for resistive modes and $d/a = 1.254$ for ideal modes.

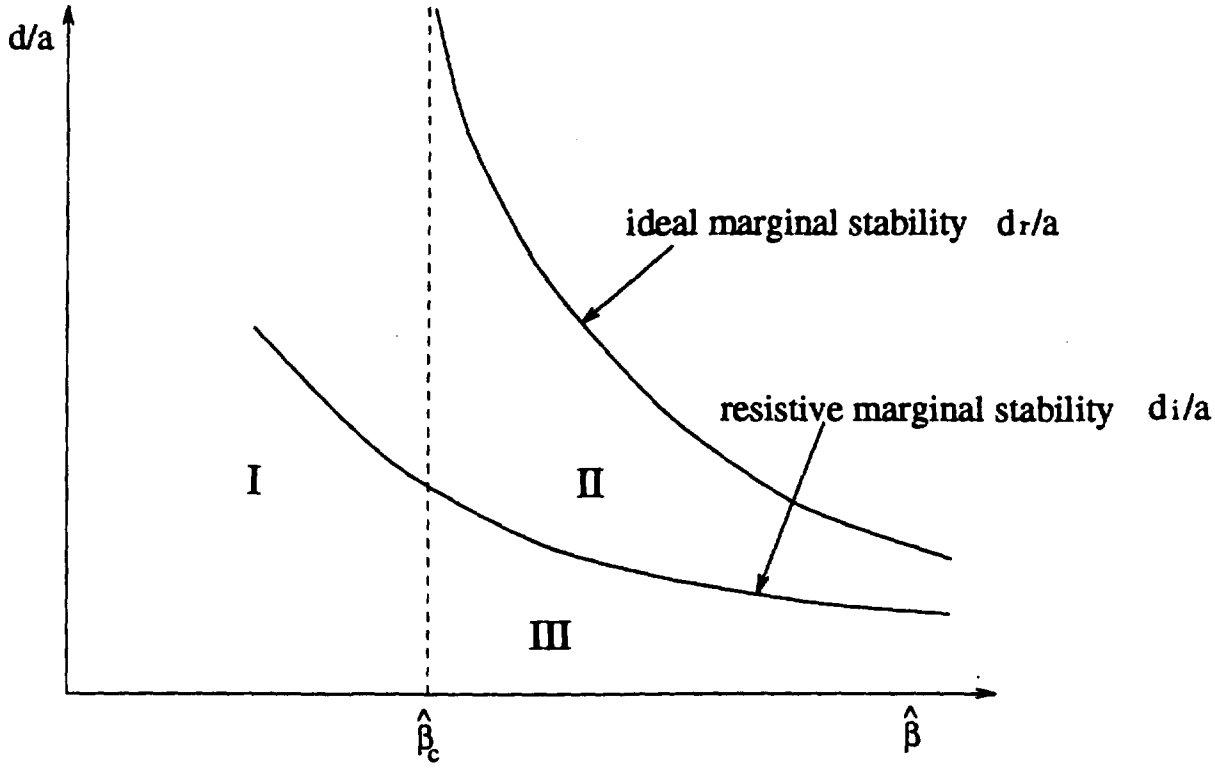
d/a
ideal marginal stability d_r/a
resistive marginal stability d_i/a
I
II
III
$\hat{\beta}_c$
$\hat{\beta}$

Figure 1:

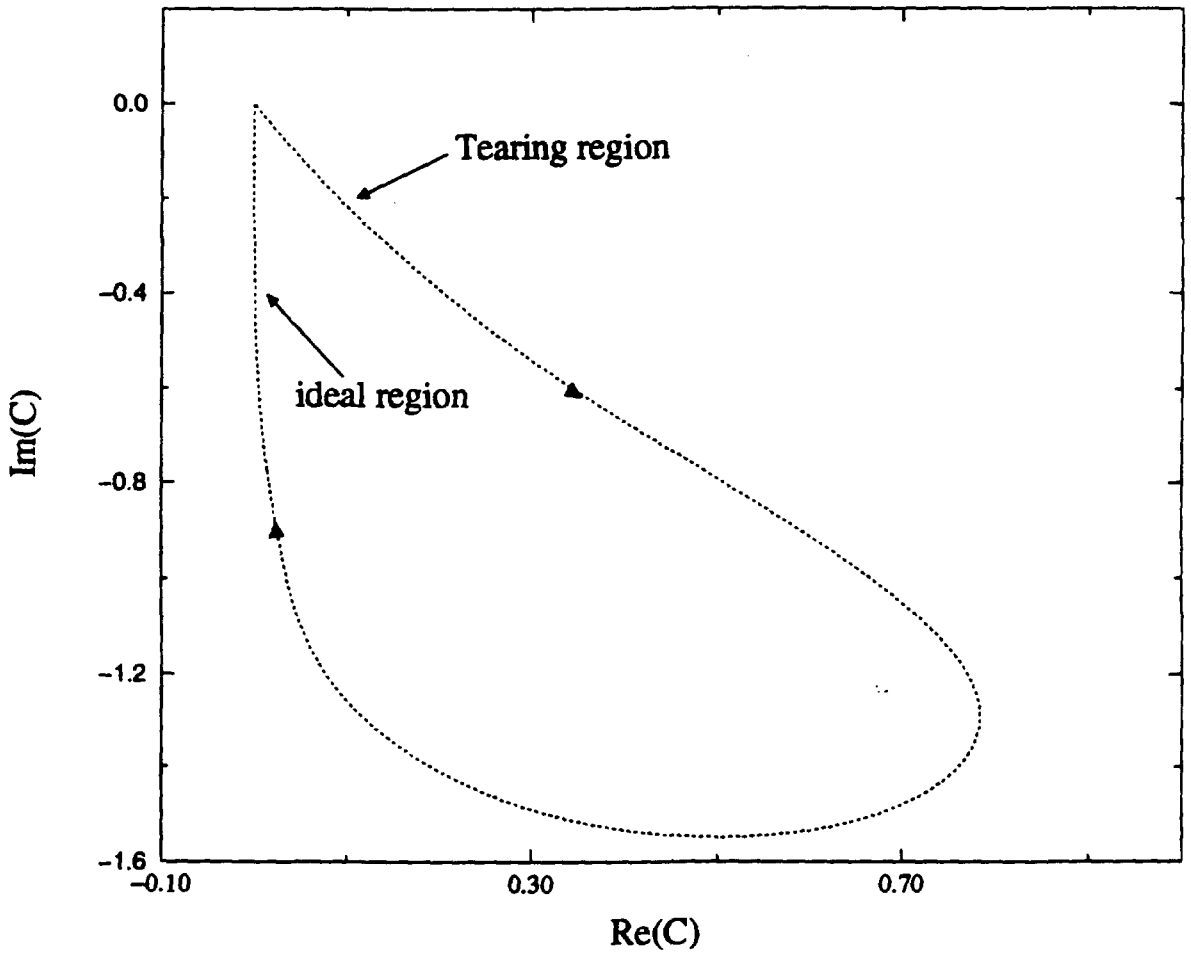

Figure 2

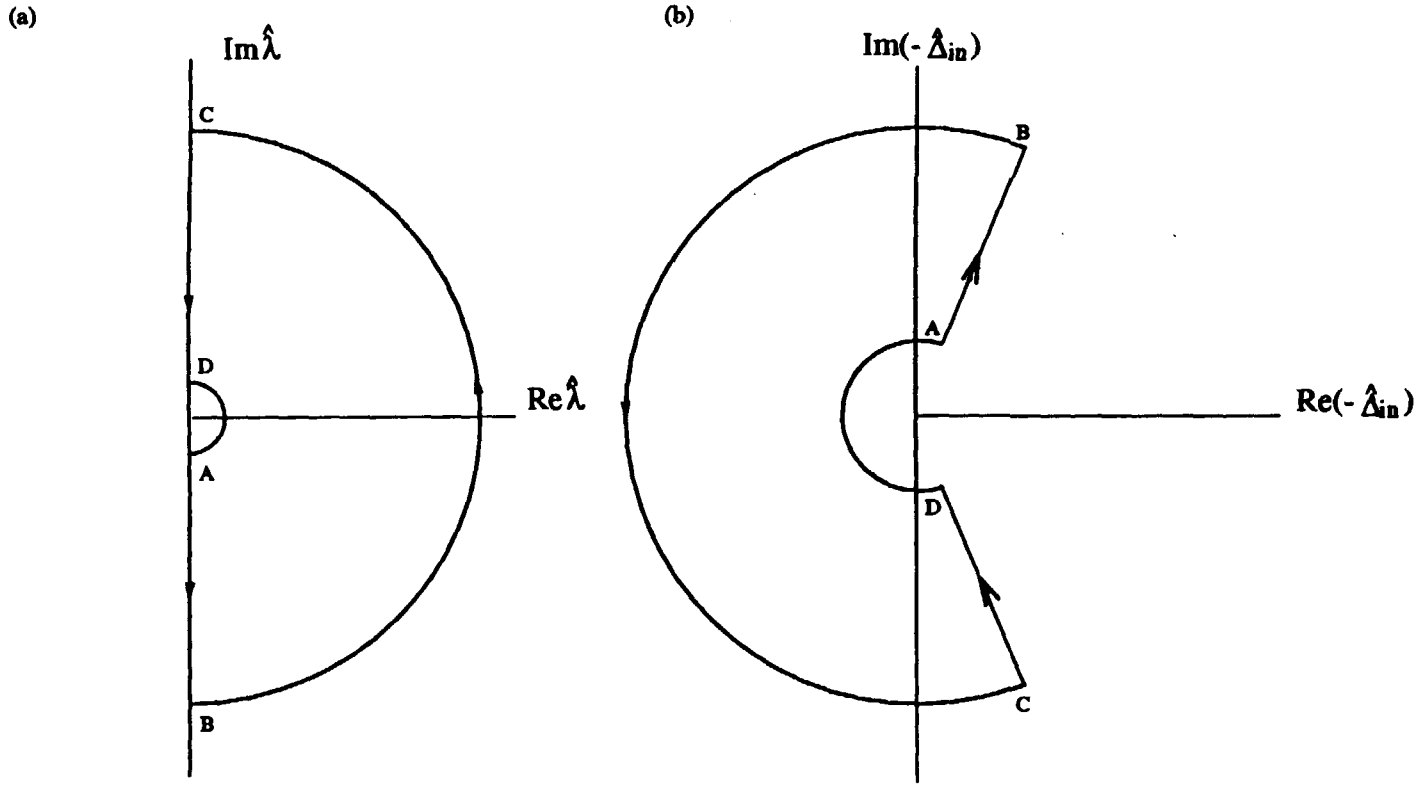
(a)
Im$\hat{\lambda}$
C
D
A
B
Re$\hat{\lambda}$
(b)
Im(- $\hat{\Delta}_{in}$)
B
A
D
C
Re(- $\hat{\Delta}_{in}$)

Figure 3

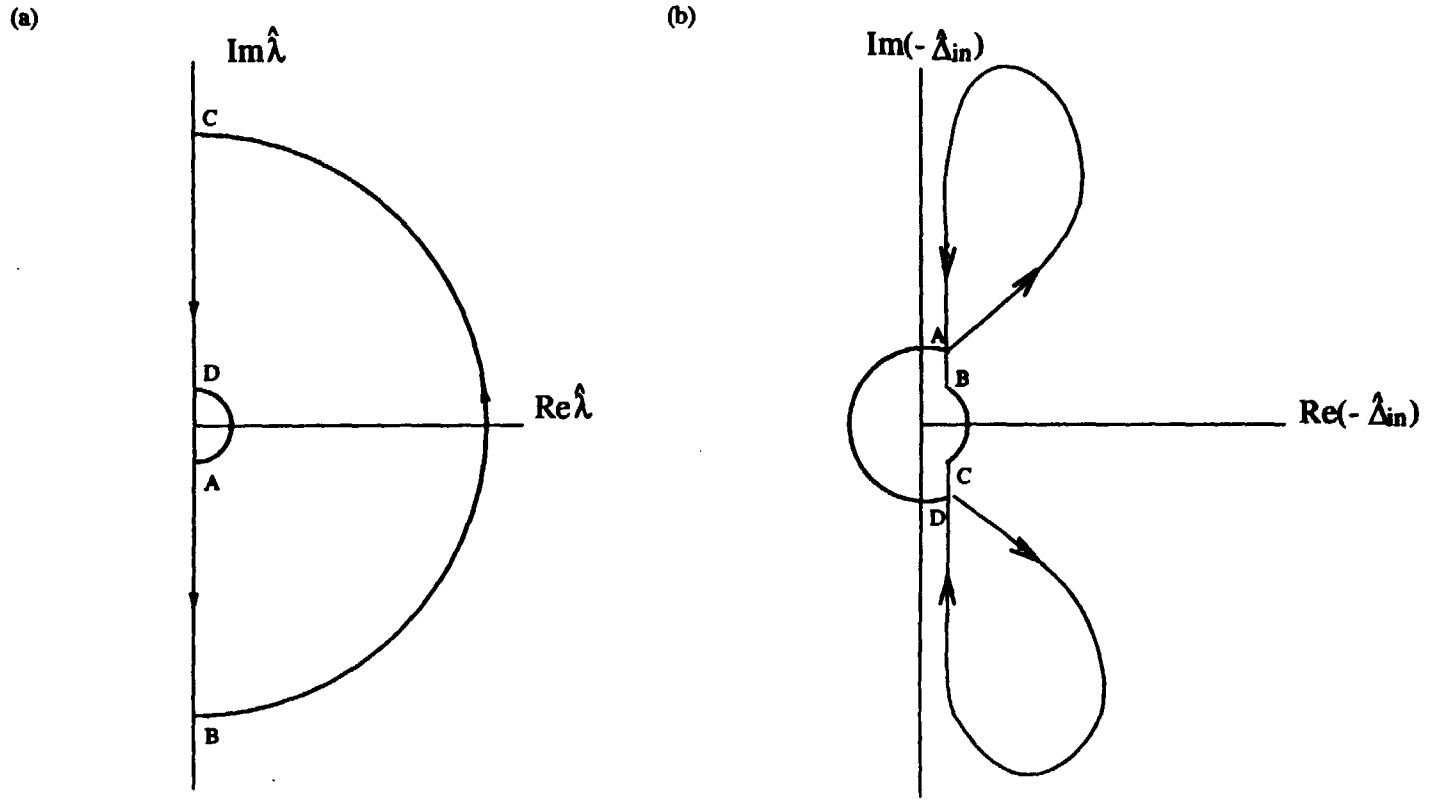
(a)
Im$\hat{\lambda}$
C
D
A
B
Re$\hat{\lambda}$
(b)
Im(- $\hat{\Delta}_{in}$)
A
B
C
D
Re(- $\hat{\Delta}_{in}$)

Figure 4

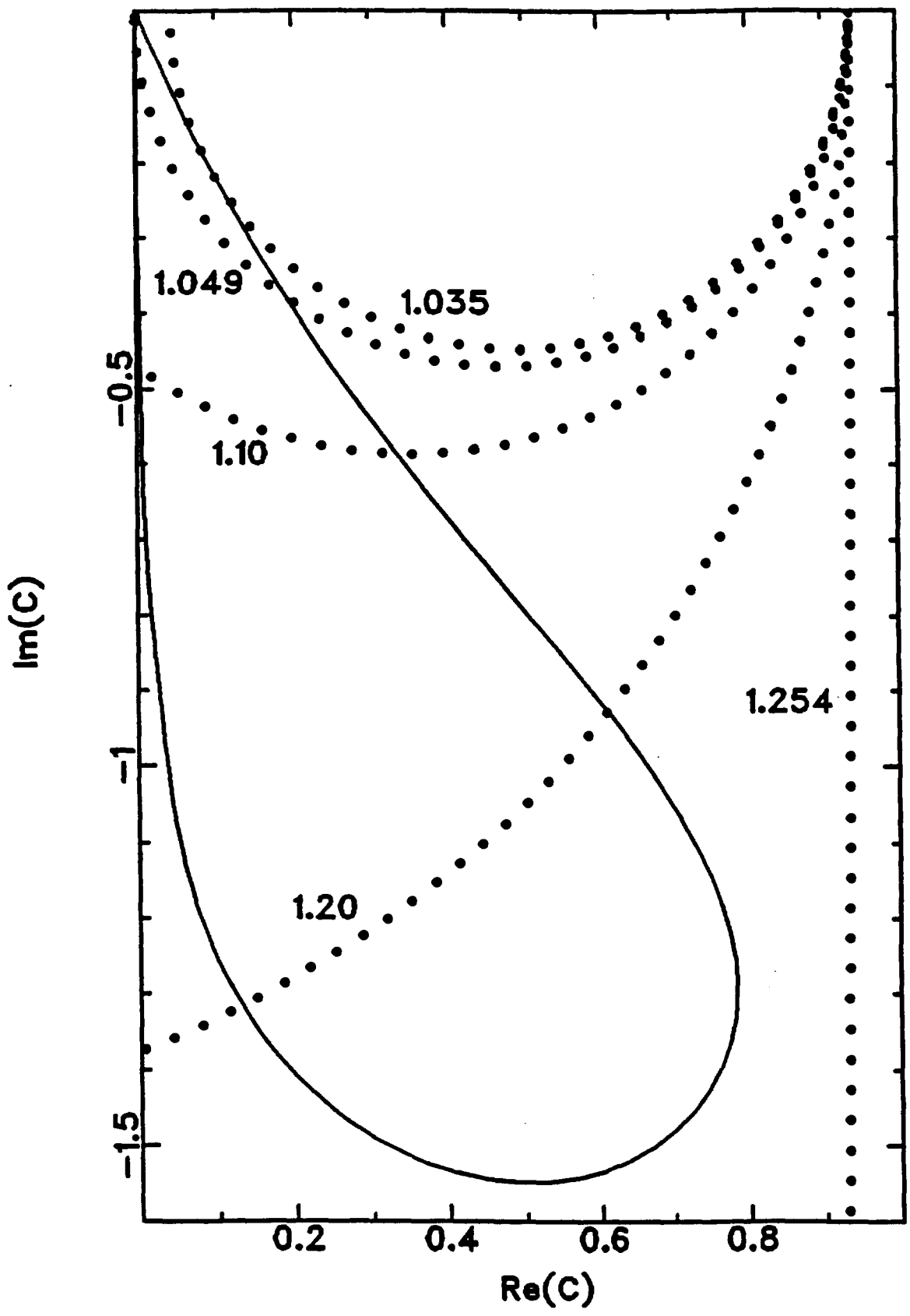

Figure 5